International Journal of Scientific Research in Science and Technology
Print ISSN: 2395-6011 | Online ISSN: 2395-602X (www.ijsrst.com)
doi : https://doi.org/10.32628/IJSRST22956

Study of Fabry-Perot Cavity Design and Radiation Features of The Antenna

Kunjesh Kumar[1], Dr. K. B. Singh[2], Dr. Rajendra Prasad[3]
[1]Department of Electronics, B. R. A. Bihar University, Muzaffarpur, Bihar, India
[2 & 3]P. G. Department of Physics, L. S. College, Muzaffarpur, B. R. A. Bihar University, Muzaffarpur, Bihar, India.

Article Info
Volume 9, Issue 5
Page Number : 64-70
Publication Issue
September-October-2022
Article History
Accepted : 01 Sep 2022
Published : 08 Sep 2022

ABSTRACT
In this present paper we studied about the Fabry Perot cavity design and radiation features of the antenna.

Keywords: Antenna, Metal Strip Grating, Fabry-Perot Cavity, Microstripline.

I. INTRODUCTION

In this paper we present the model is based on the use of a transverse equivalent network (TEN) to represent the fields in the FPC structure. This is useful to derive and explain the peculiar features of the analyzed structure. For periodic leaky-wave antennas that radiate from a higher-order space harmonic [1-3] the period is not small relative to a wavelength and such a homogenization is not possible.

II. METHODS AND MATERIAL

2.1. FABRY-PEROT CAVITY DESIGN

An FPC antenna can generally be regarded as a leaky parallel-plate waveguide excited by a finite source. The upper plate, either in the form of a dielectric screen or of a patch or slot array, allows radiation to leak out of the region between the parallel plates. To achieve a wide effective antenna aperture, and hence a directive radiation pattern, the leakage rate should be small; this is the case if, the upper plate has a low transmission coefficient. This happens when the equivalent susceptance of the upper FPC screen is much larger than the characteristic admittance. Assuming that the susceptance tends to infinity, an approximate design equation for the antenna thickness can be derived in order to achieve directive radiation at a given angle [1-5]

$$\frac{h}{\lambda_0} = \frac{0.5}{\sqrt{\varepsilon_r - \sin^2\theta_p}} = \frac{0.5}{\cos\theta_p} \quad (1)$$

Here the last expression holds for the case considered here in which, the relative dielectric constant of the medium filling the parallel-plate region, is equal to one. A more refined analysis, which takes into

account the finite value shows that in the planes the following relation holds:

$$\cot(k_{z0}h) \simeq \frac{B_{\mathrm{S}}}{Y_{\mathrm{c0}}} \tag{2}$$

Where the characteristic admittance refers to the equivalent transmission lines associated to the polarizations [6]; in the plane. The particular spatial dispersion of the MSG is such that the dependence of and on the wavenumber is the same; hence, the right-hand side in equation (1) has the same value in the principal planes. This crucial fact implies that a unique antenna thickness can be found that produces a scanned beam at the same angle in the principal planes. A high degree of azimuthal omnidirectionality of the resulting radiation pattern can then be expected. Interesting correlations exist between the problem of radiation from the considered MSG FPC antenna and the behavior of the same structure under plane-wave incidence. It can be verified that the condition of zero phase for the plane-wave reflection coefficient at the MSG plane is exactly given by (1); therefore, by the above-mentioned symmetry, the MSG above a ground plane behaves as a high-impedance surface at the same frequency in both principal planes, for both inductive and capacitive Far-Field Pattern. The component of the electric far field is written as:

$$E_p^{\mathrm{ff}}(\theta,\phi) = E_x^{\mathrm{pw}}(0,0,z_{\mathrm{s}}) \quad \text{----------} \quad 3$$

$$E_{\mathrm{co}}^{\mathrm{ff}} = f(\theta)\left(\cos\theta\cos^2\phi + \sin^2\phi\right) \quad \text{----------} \quad 4$$

$$E_{\mathrm{cross}}^{\mathrm{ff}} = f(\theta)\,(\cos\theta - 1)\sin\phi\cos\phi. \quad \text{----------} \quad -5$$

At any elevation angle, the cross-polarized component is identically zero in the principal plane. Since these are symmetry planes. At any aspect ratio, the co-to-cross polarization ratio, defined as:

$$R = \left|\frac{E_{\mathrm{co}}^{\mathrm{ff}}}{E_{\mathrm{cross}}^{\mathrm{ff}}}\right| \quad \text{----------} \quad 6$$

can be calculated from (6) in closed form as a function of the spherical angles

$$R = \left|\frac{\cos\theta\cos^2\phi + \sin^2\phi}{(\cos\theta - 1)\sin\phi\cos\phi}\right| . \quad \text{----------} \quad 7$$

The factor in (4) cancels out in (7), hence we get the remarkable result that the co-to-cross polarization ratio of the considered antenna does not depend on frequency nor on any of the physical parameters of the structure and it coincides with that of an elemental dipole in free space. The fact that there is cross polarization for an elemental dipole in free space is a consequence of the definition employed. If we had used Ludwigs second definition instead [7], the cross polarization would be zero. The third definition corresponds to that which is more commonly measured in practice. The angular range for where is larger than a prescribed value can then be determined in each elevation plane.

$$\cos\theta > \frac{R_{\min}\sin\phi\cos\phi - \sin^2\phi}{\cos^2\phi + R_{\min}\sin\phi\cos\phi} . \quad \text{----------} \quad 8$$

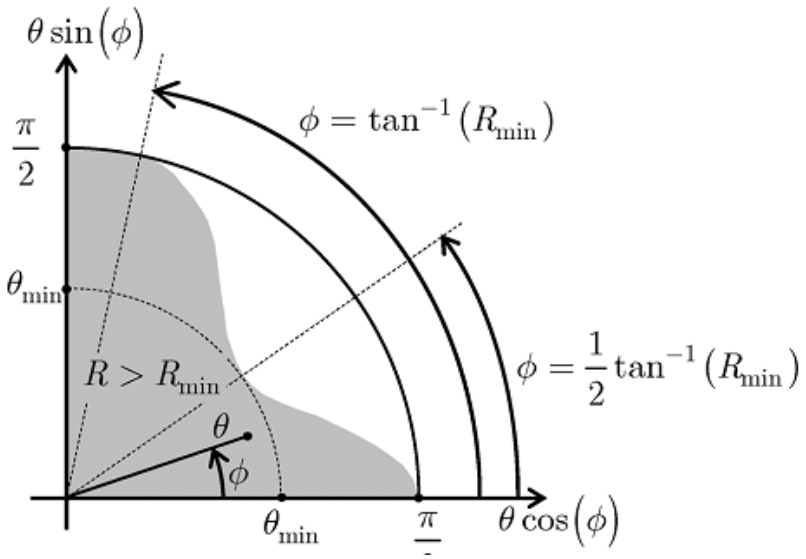

Fig. 1. Illustration of the angular region in the quadrant where the co-to-cross polarization ratio is larger than (shaded area).

A straightforward analysis of (8) shows that is larger than for all angles in the angular region, whereas for it gives.

$$\theta < \cos^{-1}\left(\frac{R_{\min}\sin\phi\cos\phi - \sin^2\phi}{\cos^2\phi + R_{\min}\sin\phi\cos\phi}\right). \quad \text{---------- 9}$$

From (8) it is found that the minimum value for is achieved in the elevation plane .

$$\theta_{\min} = \cos^{-1}\left(\frac{\sqrt{R_{\min}^2+1}-1}{\sqrt{R_{\min}^2+1}+1}\right). \quad \text{---------- 10}$$

2.2. R ADIATION FROM A HORIZONTAL ELECTRIC DIPOLE

The radiation features of the antenna shown in Fig. 1 are illustrated by providing numerical results for a specific structure with parameters. The value of the thickness has been determined by maximizing at this frequency the power density radiated at broadside. To assess quantitatively the accuracy of the approximate homogenized model of the antenna, a comparison is presented between results obtained with the TEN representations based on the temporally and spatially dispersive susceptance and full-wave results obtained with the MOM in the spatial domain. Here we have assumed an infinitesimal horizontal electric dipole source in the middle of the cavity. The far field is calculated again via reciprocity by letting a plane wave impinge on the structure. The Floquet-periodicity of the field allows for a restriction of the analysis domain to a single spatial period (unit cell of the structure); the MOM Comparison at two different frequencies between the homogenized model (TEN) and the method of moments (MOM). Parameters: Legend: plane: solid lines (MOM), circles (TEN); plane: dashed lines (MoM), squares (TEN); plane: dotted lines (MoM), diamonds (TEN). then uses a periodic Greens function to enforce the electric field integral equation on the strip conductor inside the unit cell. Entire-domain basis functions of Chebyshev type with the proper edge-singularity factor have been employed and the periodic Greens function has been accelerated by using the Ewald method [8-9].

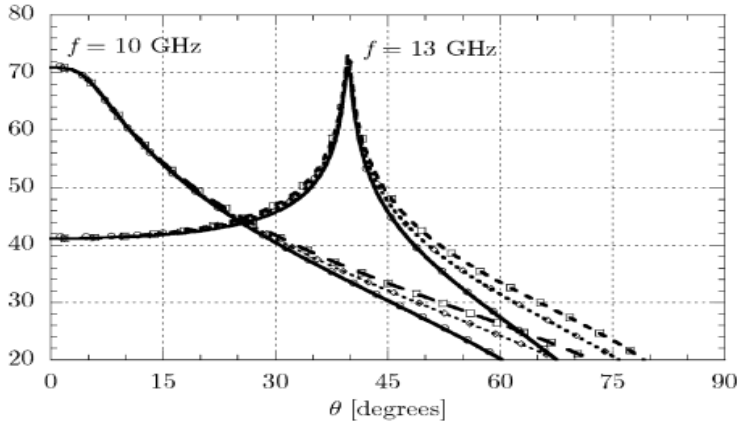

Fig. 2. Radiation patterns of the antenna in Fig. 1.

Moreover, in the MOM code the cylindrical symmetry of the structure along the strip axis is exploited to reduce the problem of plane-wave incidence from an arbitrary direction to a problem of incidence in the plane. Azimuthally Omnidirectional Radiation and Frequency Scanning Properties. In Fig. 3, far-field radiation patterns in the planes are shown for a structure as in Fig. 3. The radiated beam is seen to be scanned in elevation by varying frequency; in fact, starting from and increasing frequency, the beam opens up becoming conical in shape, with an angle of maximum radiation that covers the range from 0 to 75 in the frequency band from 10 to 35 GHz. At 30 GHz. The maximum directivity of the beams radiated at the considered frequencies are: 24.3 dBi at 10 GHz, 20.9 dBi at 11 GHz, 20.7 dBi at 13 GHz, 19.8 dBi at 20 GHz, 16.8 dBi at 30 GHz, and 14.1 dBi at 35 GHz. A s it is shown in figure 4.

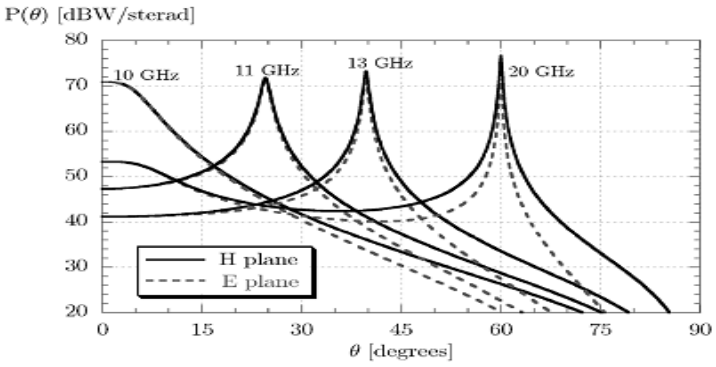

Figure 3. The directivity of the beam at different frequency

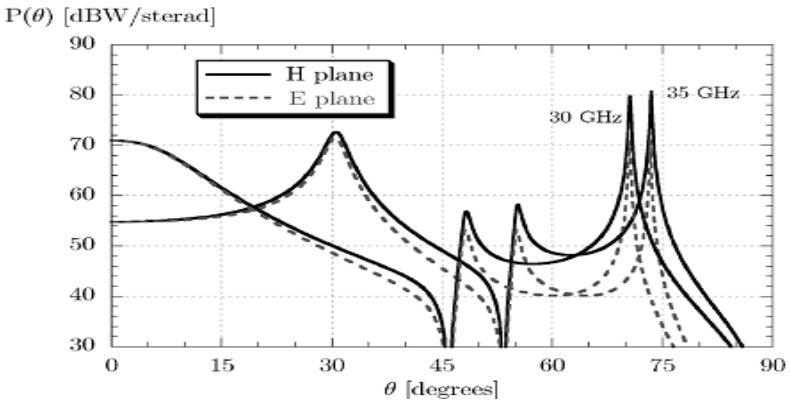

Fig. 4. Frequency scanning of the beam radiated in the planes for an MSG FPC antenna

It can be observed that, at each of the considered frequencies, the direction of maximum radiation is the same in the planes. The degree of azimuthal omnidirectionality of the radiation pattern can be appreciated from the exact values over the entire radiation sphere.

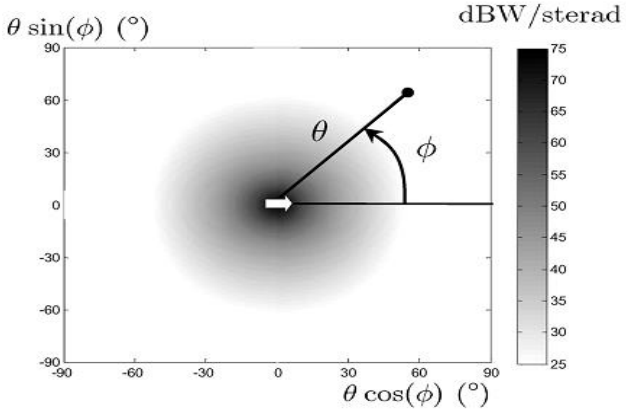

Figure 5.
Gray scale representation of the radiation pattern of an MSG –FPC Antenna
F= 10 GHZ Broad side beam θp=0

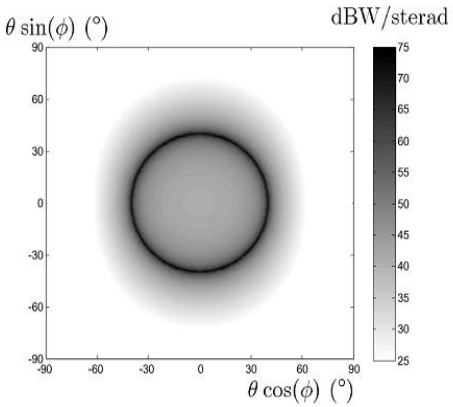

Figure 6.
Gray scale representation of the radiation pattern of an MSG –FPC Antenna
F= 13 GHZ Broad side beam, $\boldsymbol{\theta p = 39.7}$

The two properties (circular conical beam shape and constant beam width) are peculiar features of the MSG geometry, and it is not possessed by other designs of FPCs based on FSS-like PRSs. As concerns the peak intensity, in the plane it remains con-As concerns the peak intensity, in the plane it remains constant as the frequency is increased [10].

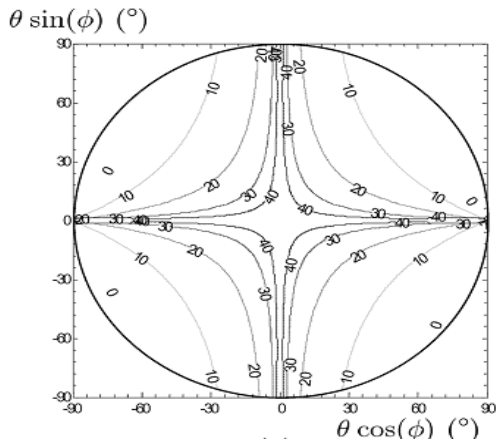

Figure 7.

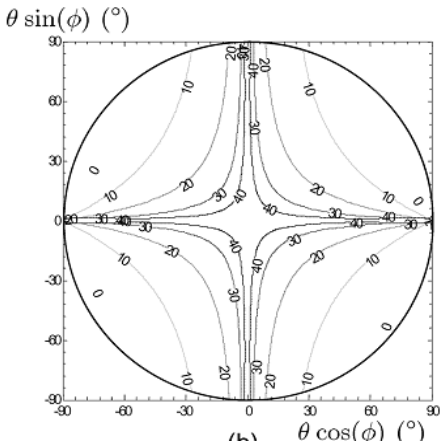

Figure 8.

2.3. POLARIZATION PROPERTIES

The polarization features of the considered FPC antenna are illustrated by adopting the same polar scale as in Fig. 6 and displaying contour plots of the co-to-cross polarization ratio (in dB), defined in (10), calculated with the MoM approach. In Fig. 7, the case of a broadside beam is considered, at; in Fig. 7, the case of a scanned beam is considered, at (corresponding to a scan angle). A very good polarization purity of the far field can be observed. Remarkably, Fig. 7 and 8 are indistinguishable: in fact, as expected from the analysis. the cross-polarization performance of the considered antenna is independent of frequency, and hence is the same for broadside and scanned beams, and is the same as that

exhibited by a horizontal elemental dipole radiating either in free space or above a ground plane [11].

III. CONCLUSIONS

A Fabry-Perot cavity antenna comprised of an MSG above a ground plane excited by a horizontal electric dipole has been studied by means of rigorous full-wave simulations. Remarkable omnidirectionality and polarization purity of the directive radiation patterns have been studied. due to the excitation of a single leaky mode along the antenna aperture that propagates omnidirectionally and has current flow only in the direction. This makes the considered MSG unique among the class of partially-reflecting surfaces employed in this type of antenna. An accurate equivalent network has also been adopted to model the antenna, based on the representation of the grating through an equivalent homogenized admittance that is both temporally and spatially dispersive. The particular dependence of such admittance on the spatial wavenumbers is shown to be the key element in establishing the peculiar observed radiation properties. From a mathematical point of view, such a dependence is related to the underlying geometric properties of the grating, which is uniform along the -direction, whereas it is periodic along the orthogonal -direction. These symmetries are shared with the wire-medium slab considered which shows similar radiation properties. The continuous translational symmetry of the structure is responsible for the occurrence of spatial dispersion, which manifests itself in a special dependence of the relevant homogenized parameters on the wavenumber. From a physical point of view, the continuous translational symmetry of the MSG, together with the gaps between the strips, allows the MSG to act as a linearly-polarized phased current sheet.

IV. REFERENCES

[1]. G. von Trentini, partially reflecting sheet arrays, IRE Trans. Antennas Propag., vol. AP-4, pp. 666671, Oct. 1956.

[2]. D. R. Jackson and N. G. Alexpoulos, Gain enhancement methods for printed circuit antennas, IEEE Trans. Propag., vol. AP-33, no. 9, pp. 976987, Sep. 1985.

[3]. A. P. Feresidis, G. Goussetis, S. Wang, and J. C. Vardaxoglou, Artificial magnetic conductor surfaces and their application to low profile high-gain planar antennas, IEEE Trans. Antennas Propag., vol. 53, no. 1, pp. 209215, Jan. 2005.

[4]. G. Lovat, P. Burghignoli, F. Capolino, and D. R. Jackson, High directivity in low-permittivity metamaterial slabs: Ray-optic vs. leaky wave models, Microwave Opt. Techn. Lett., vol. 48, no. 12, pp. 25422548, Dec. 2006.

[5]. R. Honey, A flush-mounted leaky-wave antenna with predictable patterns, IEEE Trans. Antennas Propag., vol. AP-7, no. 4, pp. 32029, Oct. 1959.

[6]. K. L. Klohn, R. E. Horn, H. Jacobs, and E. Freibergs, Silicon waveguide frequency scanning linear array antenna, IEEE Trans. Microw. Theory Tech., vol. MTT-26, no. 10, pp. 764773, Oct. 1978.

[7]. M. Guglielmi and G. Boccalone, A novel theory for dielectric-inset waveguide leaky-wave antennas, IEEE Trans. Antennas Propag., vol. 39, no. 4, pp. 497504, Apr. 1991.

[8]. Y. Kaganovsky and R. Shavit, Analysis of radiation from a line source in a grounded dielectric slab covered by a metal strip grating, IEEE Trans. Antennas Propag., vol. 57, no. 1, pp. 135143, Jan. 2009.

[9]. G. Lovat, P. Burghignoli, F. Capolino, D. R. Jackson, and D. R. Wilton, High-gain omnidirectional radiation patterns from a metal strip grating leaky-wave antenna, in IEEE AP-S

Int. Symp. Antennas Propag. Digest, Honolulu, HI, Jun. 1015, 2007, pp. 57975800.

[10]. P. Burghignoli, G. Lovat, F. Capolino, D. R. Jackson, and D. R. Wilton, Modal propagation and excitation on a wire-medium slab, IEEE Trans. Microw. Theory Tech., vol. 56, no. 5, pp. 11121124, May 2008.

[11]. T. Zhao, D. R. Jackson, J. T. Williams, and A. A. Oliner, General formulas for 2-D leaky-wave antennas, IEEE Trans. Antennas Propag., vol. 53, no. 11, pp. 35253533, Nov. 2005.

Cite this article as :

Kunjesh Kumar, Dr. K. B. Singh, Dr. Rajendra Prasad, "Study of Fabry-Perot Cavity Design and Radiation Features of The Antenna ", International Journal of Scientific Research in Science and Technology (IJSRST), Online ISSN : 2395-602X, Print ISSN : 2395-6011, Volume 9 Issue 5, pp. 64-70, September-October 2022. Available at doi : https://doi.org/10.32628/IJSRST22956
Journal URL : https://ijsrst.com/IJSRST22956